Carcinogenesis vol.11 no.8 pp.1313–1322, 1990

Diaplacental induction by ethylnitrosourea of tumours at the pial border of the central nervous system in (T × HT)F1 mice

Wolfgang Schmahl, Arne Luz, Maria Leierseder-Bauer and Angelika Neuhäuser-Klaus[1]

GSF-Institut für Pathologie and [1]GSF-Institut für Säugetiergenetik, D-8042 Neuherberg, FRG

Ethylnitrosourea (ENU) was diaplacentally applied to (T × HT)F1 mice at a dose of 40 mg/kg on different gestation days during organogenesis and early fetal stages by i.p. injection to the dams. The animals were particularly sensitive to induction of tumours at the central nervous system (CNS)–skull–vertebra interface (30 and 20% in ENU-treated male and female offspring respectively, compared with 1% in controls). ENU treatment during the late organogenesis stage (gestation days 8–11) proved to be less efficient in tumour induction than during the subsequent early fetal period (gestation days 12–14). Ninety-two per cent of the CNS tumours were located at the interface between the CNS and the osseous surrounding. The distribution of these tumours at the pial border was inhomogeneous: 69% were found at the brain–skull border, 6% of the tumours occurred within the cervico-thoracal districts and 25% within the lumbo-sacral districts of the spinal cord–vertebra interface. Histological classification revealed a preferential occurrence of neuroepithelial tumours in male offspring (~20%) and only ~7% Schwann cell tumours and ~3% tumours of meningo-mesenchymal origin. In female offspring neuroepithelial tumours and Schwann cell tumours were observed at about an equal rate (9–10%), in contrast to meningo-mesenchymal tumours (1%). Nearly 98% of these tumours were situated at the basal districts of the space between the CNS–skull and spinal cord–vertebra. This indicates a particular sensitivity of the basal neurothelium, a derivative of neural crest cells, for ENU-induced carcinogenesis. The pluripotency of these cells during the mid-gestation period apparently enables growth of different histopathological tumour types, which arise independently from each other.

Introduction

Many studies have been performed with several strains of rats to study nervous system tumours induced by ethylnitrosourea (ENU*), a model carcinogen during the perinatal period (1). However, in most experiments mice proved not to be useful in neurocarcinogenesis studies as this species lacks nearly all neurotropic action of alkylnitrosoureas (2). In a previous report (W.Schmahl *et al.*, submitted) we described the usefulness of the T × HT cross for a simultaneous study of both mutagenic and carcinogenic effects *in vivo*. In response to embryo-fetal ENU application, these mice developed not only a broad spectrum of tumours in many organs and tissues, but also, and above all, tumours in the interface between the central nervous system (CNS) and its mesenchymal surroundings. This target site is histogenetically closely related to the neural crest and thus corresponds to the main target tissue of mutagenic events characterized by coat colour spots (W.Schmahl *et al.*, submitted). The present report provides a detailed analysis of the pathohistology of tumours of the CNS.

Materials and methods

Strains

The experiments were performed on (T × HT)F1 mice heterozygous for seven recessive coat colour alleles (3). Treatment of the mice *in utero* occurred during the time of migration of the melanocyte precursor cells from the neural crest to the dermis. The alteration or loss of a wild-type allele at one of the heterozygous coat colour loci in the melanocyte precursor cells leads to the expression of the recessive allele. The resulting mutant clone can be first observed at 2 weeks of age as a coat colour spot in the developing fur.

ENU

1-Ethylnitrosourea was supplied under nitrogen oxide by Serva (Heidelberg, FRG). Immediately before i.p. injection into the pregnant females, ENU was dissolved in Sorensen buffer at pH 6.0.

Experimental procedure

The procedure has already been described in detail in a recent paper (W.Schmahl *et al.*, submitted). Briefly, virgin T stock females were mated to HT stock males and were examined for vaginal plugs during the next four mornings. The day of plug detection represents day 1 of embryonic development. ENU treatment was performed on one day of the period between days 8 and 14 of gestation. In a second series of experiments, a dose–effect study was carried out by i.p. injection of 0, 10, 20 or 40 mg/kg ENU into mice on gestation day 12.

Intraperitoneal applications were performed consistently between 9 a.m. and 11 a.m. After the litters were born, they were counted and sexed and examined for abnormalities of the extremities and the tail.

Long-term study. The mice were kept in type 2 cages (five animals) under standardized conditions. They remained in air-conditioned animal rooms at 23°C with artificial light from 6 a.m. to 6 p.m. The animals received Altromin pellets and water *ad libitum*. Systematic observations were conducted on 5 days a week. All animals with neurologic symptoms, severely reduced activity, dyspnoe or palpable tumours, as well as those with deformities of the skull, were autopsied. Autopsies were also performed on cases of spontaneous death. After registration of macroscopic findings, all abnormalities were also studied in histological sections. In particular, the head region was studied histologically as a whole whenever findings were established by X-ray examination (breaking of the skull sutures) and in the case of brain atrophy or hydrocephalus externus. Histopathology routinely included coronal sections (i) at the planes between the area frontalis and the area parietalis of the cortex cerebri, (ii) at the mammillary region and (iii) at the region of the mesencephalic nuclei.

Histological evaluation

After an adequate fixation period in 4% buffered formalin the specimens were embedded in paraffin and 6 μm thick sections were produced. These were routinely stained with haematoxylin and eosin, van Gieson and PAS.

Despite the difficulties in attributing tumour components to distinct histogenetic pathways, it was necessary to establish a practical classification scheme from human pathology (4), as well as from the pathology of the laboratory rat (5). It was decided to use three main categories depending on the most conspicuous part of each tumour. This classification was performed independently by two of the investigators. Since we reached a high degree of conformity in our diagnoses, our impression was strengthened that only a few tumours could potentially be listed under different items at the same time. The precise immunohistochemical classification of the tumours is the subject of a forthcoming publication.

Statistical evaluation

The time of observation was arbitrarily divided into 50 day periods. This score was composed of those animals suffering from tumours of the CNS periphery

---

*Abbreviations: ENU, ethylnitrosourea; CNS, central nervous system; g.d., gestation day.

(tumours of the brain–skull and the spinal cord–vertebra interfaces) according to their age at autopsy. To recognize significant differences between tumour incidences, a contingency table analysis was performed (Fisher test).

Results

General tumour frequency

This subject has been presented in another report (W.Schmahl *et al.*, submitted). The present communication concerns tumours of the CNS and tumours at the border between neuroectoderm and its mesenchymal surrounding.

Frequency of tumours of the CNS and related tissues (Tables I and II)

Tumours originating within the CNS parenchyme. Eighteen genuine tumours of the CNS (2.6%) were registered in treated male offspring, and 12 tumours (1.8%) were found in females within the CNS parenchyme, revealing no connection to the pial border zone. In controls no similar tumours were observed.

Tumours in the dural space of the CNS. Tumours of this location occurred only rarely in control animals (0.8% in males; 0.5% in females). After ENU treatment, tumours of the CNS–skull–vertebra interface were observed in 27.9% of the males and 18.6% of the females ($P < 0.0001$) (Tables I and II). In this group, seven males and six females also had a genuine tumour of the CNS parenchyme (Tables III and IV, column 6). The dural space tumours constantly infiltrated into the neighbouring CNS parenchyme and less frequently into the osseous surroundings. We do not yet have any indication that the latter tissues represent the primary ENU targets from which the border zone tumours have originated. The main induction period in both sexes was between gestation day (g.d.) 10 and 14 with a marked peak on g.d. 13 in male offspring (49.1% frequency) and female offspring (30.6%) (Tables I and II). The high sensitivity of this gestation day was also documented by a tumour multiplicity of 1.34 in males and 1.21 in females (Tables III and IV). In contrast, mean tumour multiplicity was 1.16 in males and 1.12 in females.

The induction of these tumours follows a dose–effect relationship in both sexes, but this was most evident in females (Tables I and II). Although the treatment groups 12/40/1 and 12/40/2 received identical doses, the ENU came from different batches and experiments were separated by several months, the resulting tumour frequencies being markedly different in females.

Table I. Animals with tumours of the nervous system and related tissues in male (T × HT) offspring after ENU treatment on different gestation days (numbers and per cent)

	ENU treatment g.d./dose (mg/kg)											
	0 (controls)	8/40	9/40	10/40	11/40	12/40/1	13/40	14/40	12/10	12/20	12/40/2	All treatments
No. of animals observed	243	45	49	94	77	56	110	35	101	72	66	705
1. Tumours of the CNS parenchyme	(0)	(0)	(1) 2.0	(1) 1.1	(2) 2.6	(2) 3.6	(3) 2.7	(2) 5.7	(3) 3.0	(0)	(4) 6.1	(18) 2.6
2. Tumours of the CNS–skull–vertebra interface	(2) 0.8	(0)	(1) 2.0	(25) 26.6	(28) 36.4	(20) 35.7	(54) 49.1	(9) 25.7	(20) 20.0	(18) 25.0	(22) 33.3	(197) 27.9
3. Tumours of the nervus V	(1) 0.4	(0)	(0)	(0)	(1) 1.3	(1) 1.8	(4) 3.6	(0)	(1) 1.0	(0)	(2) 3.0	(9) 1.3
4. Tumours of the peripheral nervous system	(0)	(0)	(0)	(4) 4.3	(1) 1.3	(2) 3.6	(1) 0.9	(0)	(0)	(1) 1.4	(0)	(9) 1.3
5. Hyperplastic lesions of the cranial meninges	(1) 0.4	(0)	(1) 2.0	(1) 1.1	(2) 2.6	(1) 1.8	(2) 1.8	(0)	(0)	(2) 2.8	(0)	(9) 1.3

Table II. Animals with tumours of the nervous system and related tissues in female (T × HT) offspring after ENU treatment on different gestation days (numbers and per cent)

	ENU treatment g.d./dose (mg/kg)											
	0 (controls)	8/40	9/40	10/40	11/40	12/40/1	13/40	14/40	12/10	12/20	12/40/2	All treatments
No. of animals observed	215	44	54	86	71	40	108	18	105	70	72	668
1. Tumours of the CNS parenchyme	(0)	(0)	(0)	(0)	(5) 7.0	(1) 2.5	(2) 1.9	(1) 5.6	(0)	(1) 1.4	(2) 2.8	(12) 1.8
2. Tumours of the CNS–skull–vertebra interface	(1) 0.5	(1) 2.3	(2) 3.7	(6) 7.0	(13) 18.3	(10) 25.0	(33) 30.6	(4) 22.2	(11) 10.5	(14) 20.0	(30) 41.7	(124) 18.6[a]
3. Tumours of the nervus V	(0)	(0)	(0)	(0)	(0)	(2) 5.0	(6) 5.6	(0)	(0)	(0)	(0)	(8) 1.2
4. Tumours of the peripheral nervous system	(0)	(0)	(0)	(2) 2.3	(1) 1.4	(2) 5.0	(5) 4.6	(5) 27.8	(0)	(2) 2.9	(2) 2.8	(19) 2.8
5. Hyperplastic lesions of the cranial meninges	(0)	(0)	(2) 3.7	(2) 2.3	(2) 2.8	(1) 2.5	(7) 6.5	(0) 0	(1) 0.9	(1) 1.4	(4) 5.6	(20) 3.0

[a] Significant compared to the incidence in male offspring, $P < 0.0001$.

The incidences were 25.0 and 41.7% respectively. In contrast, tumour multiplicity was quite constant in these two groups (Table II).

Tumours of the nervus trigeminus. Apart from one tumour in a male control animal, there were a few cases of these tumours in the intracranial section of the nervus trigeminus. We registered only those tumours that could be discerned clearly from other tumours of the brain–skull interface. The sensitive phase for induction was around g.d. 13 in both sexes (Tables I and II). The tumours were all classified as Schwannomas.

Tumours of the peripheral nervous system. Tumours of this type were not observed in control animals, but amounted to 1.3% in males and 2.8% in females in the ENU-exposed groups. Tumours of the peripheral nerves were histologically classified as Schwannomas. They were mostly found within the walls of the intestinal tract, and at sub-peritoneal and sub-mediastinal locations. The main induction period was from g.d. 10 to 12 in males and from g.d. 12 to 14 in females, with a distinct peak on the later day of gestation.

Fibrosis of the cranial meningeal tissue. We regarded this finding as being related to the tumorigenesis of the brain–skull interface, indicating further the sensitivity of the dural border zone for carcinogenic late effects in this strain of mice. Nodular to diffuse fibrosis occurred in one control male, but in 1.3% of the males treated. In the female offspring of treated dams an incidence of 3% was registered, with a distinct peak of inducibility around g.d. 12–13 (Tables I and II). In no case was the fibrotic alteration related to the eventual occurrence of brain tumours. For instance, in females of the 13/40 group, seven cases of meningeal fibrosis were observed, from which only two cases showed simultaneously a tumour at the basal dural space. In most cases, the lesions were seen beyond the calotte and represented well-circumscribed foci without adherence to the underlying nervous tissue.

Histological classification of the tumours

Genuine tumours of the CNS parenchyme (Tables V and VI). The most sensitive period for tumour induction in males was between g.d. 12 and 14. In female offspring we observed two induction

Table III. Frequency and multiplicity of tumours of the CNS and of the CNS–skull–vertebra interface in (T × HT)F1 males after ENU treatment on different gestation days

ENU treatment g.d./dose (mg/kg)	No. of animals with tumours			No. of tumours				
	1 Solitary CNS tumours	2 Tumours of the CNS border	3 Sum 1 + 2	4 Within CNS parenchyme	5 At the CNS border zone	6 CNS tumours simultaneous with 5	7 Sum 4 + 5 + 6	8 Multiplicity
Controls	0	0	0	0	0	0	0	0
8/40	0	0	0	0	0	0	0	0
9/40	1	1	2	1	1	0	2	1.00
10/40	0	25	25	0	27	1	28	1.12
11/40	1	28	29	1	32	1	34	1.17
12/40/1	1	20	21	1	21	1	23	1.09
13/40	1	54	55	1	71	2	74	1.34
14/40	1	9	10	1	9	1	11	1.10
12/10	3	20	23	3	20	0	23	1.00
12/20	0	18	18	0	20	0	20	1.11
12/40/2	3	22	25	3	23	1	27	1.08
Total 705	11 (1.6%)	197 (27.9%)	208 (29.5%)	11	224	7	242	1.16

Table IV. Frequency and multiplicity of tumours of the CNS and of the CNS–skull–vertebra interface in (T × HT)F1 females after ENU treatment on different gestation days

ENU treatment g.d./dose (mg/kg)	No. of animals with tumours			No. of tumours				
	1 Solitary CNS tumours	2 Tumours of the CNS border	3 Sum 1 + 2	4 Within CNS parenchyme	5 At the CNS border zone	6 CNS tumours simultaneous with 5	7 Sum 4 + 5 + 6	8 Multiplicity
Controls	0	1	1	0	1	0	1	1.00
8/40	0	1	1	0	1	0	1	1.00
9/40	0	2	2	0	3	0	3	1.50
10/40	0	6	6	0	7	0	7	1.17
11/40	3	13	16	3	13	2	18	1.12
12/40/1	1	10	11	1	10	0	11	1.00
13/40	0	33	33	0	38	2	40	1.21
14/40	0	4	4	0	4	1	5	1.25
12/10	0	11	11	0	11	0	11	1.00
12/20	0	14	14	0	16	1	17	1.21
12/40/2	2	30	32	2	31	0	33	1.03
Total 668	6 (0.9%)	124 (18.6%)	130 (19.5%)	6	134	6	146	1.12

Table V. Pattern of intraparenchymal tumours of the CNS in male (T × HT)F1 mice after ENU treatment on different gestation days

Gestation day/ENU dose (mg/kg)	Animals (nos.)	Tumours (nos) %	*Histological classification of the tumours*					*Location within*	
			Glioma/ astrocytoma	Glioblastoma	Gliosarcoma	Angioma	Melanoma	Brain	Spinal cord
Controls	243	(0) 0							
8/40	45	(0) 0							
9/40	49	(1) 2.0			1				1
10/40	94	(1) 1.1		1				1	
11/40	77	(2) 2.6	1				1	1	1
12/40/1	56	(2) 3.6	1	1				2	
13/40	110	(3) 2.7		3				2	1
14/40	35	(2) 5.7	1	1				1	1
12/10	101	(3) 3.0	1	1	1			1	2
12/20	72	(0) 0							
12/40/2	66	(4) 6.1	3	1				3	1
Total	705	(18) 2.6	7	8	2	0	1	11	7

Table VI. Pattern of intraparenchymal tumours of the CNS in female (T × HT)F1 mice after ENU treatment on different gestation days

Gestation day/ENU dose (mg/kg)	Animals (nos.)	Tumours (nos.) %	Histological classification of the tumours					Location within	
			Glioma/ astrocytoma	Glioblastoma	Gliosarcoma	Angioma	Melanoma	Brain	Spinal cord
Controls	215	(0) 0							
8/40	43	(0) 0							
9/40	54	(0) 0							
10/40	86	(0) 0							
11/40	71	(5) 7.0	1	2		2		4	1
12/40/1	40	(1) 2.5			1			1	0
13/40	108	(2) 1.9	1				1	2	0
14/40	18	(1) 5.6	1					1	0
12/10	105	(0) 0							
12/20	70	(1) 1.4	1					1	0
12/40/2	72	(2) 2.8	1	1				2	0
Total	668	(12) 1.8	5	3	1	2	1	11	1

peaks on g.d. 11 and 14 (7.0 and 5.6% respectively). They were primarily located in the brain in both sexes with a ratio of 11:7 in males and 11:1 in females for the brain/spinal cord distribution.

The most common type of tumour was the neuroepithelial tumour [oligodendroglioma, astrocytoma, glioblastoma (Figure 1), and gliosarcoma] in both sexes with a distinct preference in males after ENU treatment on g.d. 12–13.

Tumours in the dural space. Whereas the intraparenchymal tumours of the CNS were quite easy to classify due to the most abundant components, classification proved more difficult in the cases of tumours growing within the dural space. The latter were principally composed of several different cell types with a heterogenous lineage. These comprised CNS tumours of neuroepithelial origin, tumours of the nerve sheath and related tissues, as well as meningeal tumours and mesenchymal tumours of the spindle-cell type which showed a varying degree of participation within the neoplastic areas.

Tumours of neuroepithelial origin. There were either typical oligodendrogliomas or mixed oligodendro-astrocytic tumours or even anaplastic gliomas and astrocytomas, glioblastomas as well as 'primitive' neuroepithelial tumours.

The typical picture was the formation of rows, cords or rings by tumour cells with occasional palisading (Figure 1). Some areas showed a rather fibrocytic, 'stroma-like' differentiation. Van Gieson staining nevertheless hardly demonstrated any collagen in those regions.

This type of tumour was more frequently induced in males (20.9%) than in females (8.7%), with a peak after treatment on gestation day 13 in both sexes (Table VII). Its distribution within the neuraxis was fairly homogeneous. In terms of their inducibility, these tumours revealed a clear dose–response pattern.

Neuroepithelial tumours appeared as two separate clusters during the observation period (Table VIII). The first peak occurred between 200 and 350 days, the second peak beyond 450 days. Whereas in males the magnitude of these two observation clusters showed a ratio of 53:90 (37:63%), this ratio was shifted in female offspring to 10:48 (17:83%).

Tumours of nerve sheath cells and related tissues. These tumours were composed of bipolar cells with mostly elongated nuclei and intermingled areas containing bundles of compact, interweaving elongated cells, alternating with areas of looser texture. In the former parts some alignment of nuclei in parallel rows or clusters was observed and referred to as palisading. This corresponds to Antoni A-type neurilemmoma, the loosely arranged areas being defined as Antoni B-type neurilemmoma (Figure 2). These tumours were characterized by their destructive capacity at the underlying bone where they rigorously invaded the bone marrow cavities. Infiltrations of the brain and spinal cord periphery were

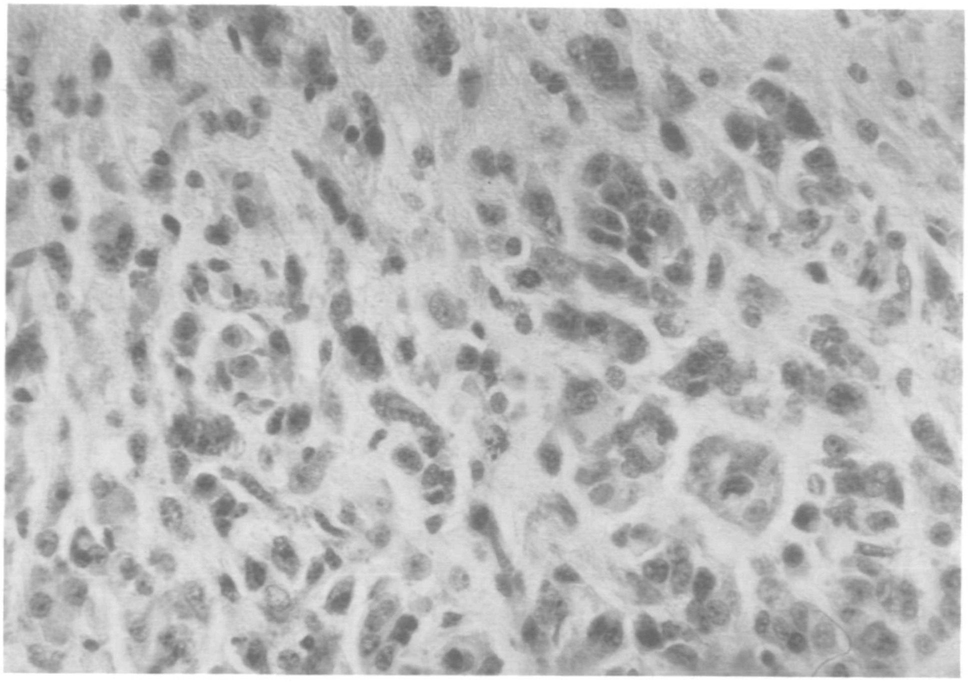

Fig. 1. Male (T × HT)F1 mouse at an age of 939 days, after ENU treatment (10 mg/kg) on g.d 12. Glioblastoma multiforme arising at the basal parts of the forebrain with infiltration of the parenchyme. H&E, ×560.

Table VII. Histological classification of tumours of the CNS–skull–vertebra interface in (T × HT)F1 mice in relation to gestation day of treatment with ENU. Classification according to the predominant (>50%) cell type (numbers and per cent)

Gestation day/ ENU dose (mg/kg)	Males					Females				
	Animals	Neuroepithelial tumours	Tumours of nerve sheath cells	Meningo-mesenchymal tumours		Animals	Neuroepithelial tumours	Tumours of nerve sheath cells	Meningo-mesenchymal tumours	
Controls	243	(0)	(1) 0.4	(1) 0.4		215	(0)	(1) 0.5	(0)	
8/40	45	(0)	(0)	(0)		43	(0)	(1) 2.3	(0)	
9/40	49	(0)	(0)	(1) 2.0		54	(2) 3.7	(0)	(1) 1.8	
10/40	94	(18) 19.1	(3) 3.2	(6) 6.4		86	(6) 7.0	(1) 1.2	(0)	
11/40	77	(23) 29.9	(6) 7.8	(3) 3.9		71	(8) 11.3	(4) 5.6	(1) 1.4	
12/40/1	56	(15) 26.8^{d}	(4) 7.1^{f}	(2) 3.6		40	(2) 5.0	(7) 17.5	(1) 2.5	
13/40	110	(49) 44.5^{d}	(20) 18.2^{f}	(2) 1.8		108	(14) 13.0	(20) 18.5	(4) 3.7	
14/40	35	(2) 5.7	(5) 14.3	(2) 5.7		18	(1) 5.6	(3) 16.7	(0)	
12/10	101	(12) 11.9	(5) 5.0	(3) 3.0		105	(4) 3.8	(7) 6.7	(0)	
12/20	72	(12) 16.7	(4) 5.6	(4) 5.6		70	(9) 12.9	(5) 7.1	(2) 2.9	
12/40/2	66	(16) 24.2	(5) 7.6	(2) 3.0		72	(12) 16.7	(19) 26.4	(0)	
					sum					sum
Total	705	(147) 20.9^{a}	(52) 7.4	(25) 3.5	224	668	(58) 8.7^{a}	(67) 10.0	(9) 1.3	134
Brain–skull interface		(79) 11.2	(46) 6.5^{b}	(18) 2.6^{e}	143		(37) 5.5	(56) 8.4^{c}	(8) 1.2	101
Spinal cord–vertebra interface		(68) 9.7	(6) 0.9^{b}	(7) 0.9^{e}	81		(21) 3.2	(11) 1.6^{c}	(1) 0.1	33

Significances between pairs of data: $^{a,b,c}P < 0.0001$; $^{d,e}P = 0.02$; $^{f}P = 0.04$.

also frequently observed. Nerve sheath tumours were found at a frequency of 7.4% in males and 10% in female offspring (Table VII). Their peak occurrence was after g.d. 13–14 in both males and females. In the females there was a great discrepancy between treatment groups 12/40/1 and 12/40/2 with respect to these tumours. There was apparently no dose–response relationship in the induction of these tumours. In addition, they were ~7 times more frequently found at the brain–skull interface than at the periphery of the spinal cord (bottom of Table VII).

Tumours of the nerve sheath showed two main clusters within the autopsy time scale in males and three clusters in females. In the former, these occurred between 250 and 350 days, a second broad cluster being established from 450 days onward (Table VIII). In female offspring a cluster of these tumours was seen in the period up to 350 days. The second peak (54%) occurred around 400–500 days. Finally, 48% of all cases of this type of tumour were observed in the period between 550 and 600 days.

Tumours of meningo-mesenchymal origin. These tumours were mostly composed of elongated spindle cells with narrow, rod-like nuclei. The cells were arranged in interlacing bundles with a tendency to whorling. However, the onion-shaped pattern typical of meningeomas was hardly observed (Figure 3). There was an abundance of collagen fibres as well as cases with many less well-defined sinusoidal blood spaces. This group also included sarcomatous tumours of the dural space where spindle-cell-shaped sarcomas predominated either as fibrosarcomas or as polymorphocellular sarcomas. The latter occurred as spindle-cell tumours with small nuclei extending mostly within the dura, infiltrating and destroying the neighbouring bone and the brain parenchyme. They often resemble both a meningotheliomatous meningioma as well as a fibrous meningioma. Spindle cell tumours occurred more frequently in males (3.5%) than in females (1.3%) (Table VII). They revealed a rather broad induction period with no outstanding peak of incidence in any experimental group. There was also no evidence of a dose–response relationship. These tumours were induced significantly more often at intracranial sites (2.6 and 1.2% in males and females respectively) than within the vertebral column (0.9 and 0.1%). Remarkably, these spindle cell tumours did not reveal any relationship in latency and differential frequencies to the occurrence of either neuroepithelial tumours or nerve sheath tumours.

Topographical distribution pattern of tumours at the CNS–skull–vertebra interface

Site specificity within the CNS circumference (all experimental groups). From the 224 dural space tumours registered in male offspring, 143 (63.8%) were located within the cranium. In females, 101 out of 134 tumours (75.4%) were found at this site (Table VII). Of this total of 244 intracranial tumours, 239 (98.3%) were located at the base of the brain, the others were found at the lateral and dorsal region of the dural space. The basally located tumours extended from the area of the nervi optici to the region of the roots of the nervus trigeminus.

The remaining 81 and 33 tumour cases within the vertebral column of males and females respectively also revealed a distinct preferential location in the ventral to ventro-lateral districts of the spinal cord. However, as these tumours had already expanded severely before the animals revealed symptoms and were autop-

Table VIII. Time scale of detection of the tumours of the CNS pial border zone within the postnatal observation period. Compilation (numbers and per cent) of tumours in (T × HT)F1 mice of all experimental groups

Histological classification of the tumours according to the predominant (>50%) cell type	Sex	Total no.	% tumours observed within the following intervals (days)									
			<250	251–300	301–350	351–400	401–450	451–500	501–550	551–600	601–650	>651
Neuroepithelial tumours	♂	147	(5) 3.4	(1) 0.7	(47) 32.0	(0) 0.0	(1) 0 7	(33) 22.4	(35) 23.8	(12) 8.2	(9) 6.1	(3) 2.0
	♀	58	(0) 0.0	(4) 6.9	(6) 10.3	(0) 0.0	(0) 0.0	(5) 8.6	(24) 41.4	(9) 15.5	(8) 13.8	(2) 3.4
Tumours of nerve sheath cells (Schwann cells)	♂	52	(0) 0.0	(13) 25.0	(3) 5 8	(0) 0.0	(0) 0.0	(5) 9.6	(11) 21.2	(5) 9.6	(11) 21.2	(1) 1.9
	♀	67	(3) 4.5	(8) 11.9	(7) 10.4	(1) 1.5	(19) 28.3	(10) 14.9	(2) 3.0	(17) 25.4	(0) 0 0	(0) 0.0
Meningo-mesenchymal tumours	♂	25	(1) 4 0	(1) 4.0	(1) 4.0	(2) 8.0	(3) 12.0	(3) 12.0	(1) 4.0	(5) 20.0	(3) 12.0	(5) 20.0
	♀	9	(0) 0.0	(0) 0.0	(3) 33.3	(2) 22.2	(2) 22.2	(0) 0.0	(1) 11.1	(1) 11.1	(0) 0 0	(0) 0.0

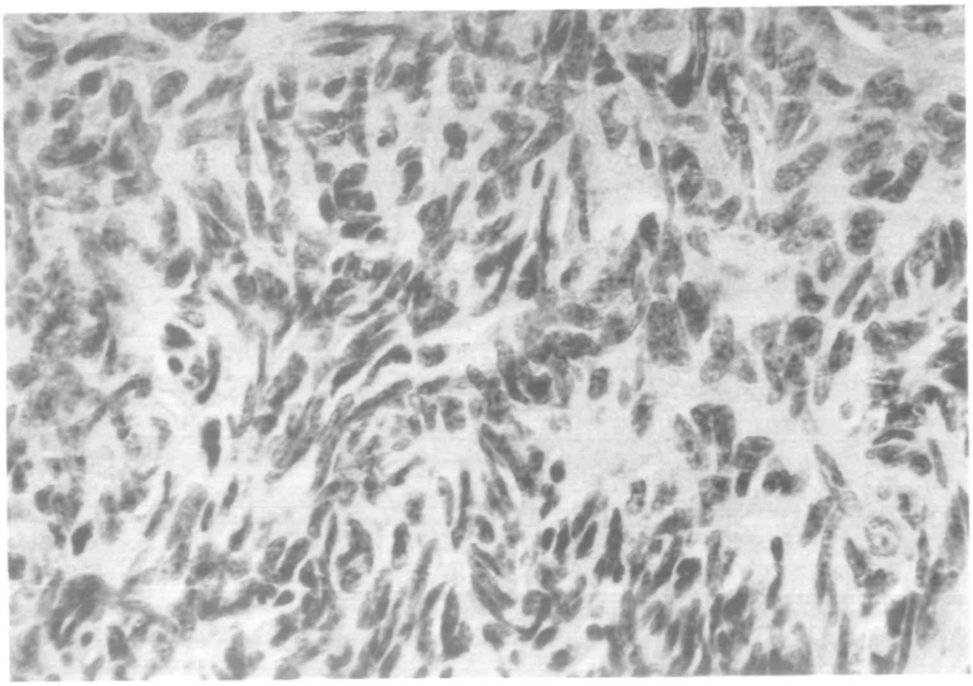

Fig. 2. Male (T × HT)F1 mouse at an age of 553 days, after ENU treatment (40 mg/kg) on g.d. 10. Malignant Schwannoma at the spinal cord border zone within cervical segments 3–4. H&E, ×875.

sied, circular growth engulfing the spinal cord circumference was also observed. An analysis of site of origin was therefore hardly possible in each case.

Site specificity across the neuraxis. This evaluation comprises only the time–response experiments with 40 mg/kg ENU. Dose-related effects are therefore excluded (Table IX).

Sixty-nine per cent of all tumours of the CNS border zone were found intracranially, 6% were located in the cervico-thoracal segments of the vertebral column and 25% in its lumbo-sacral segments. ENU treatment during organogenesis (g.d. 8–11) was less effective in the induction of tumours (16%) than the subsequent early fetal stage (41.7%, $P < 0.0001$).

The early fetal period was ~2–3 times more sensitive for induction of CNS border zone tumours than the organogenesis stage. The lumbo-sacral districts were affected almost exclusively in both sexes after treatment on g.d. 8 or 9. This was followed by the first induction of tumours at the base of the brain, which accounted for the great majority of all tumours. ENU treatment on g.d. 14 induced almost exclusively tumours at the base of the brain. In both sexes only one animal was found with a tumour in the sacral district of the spinal cord border after ENU application on g.d. 14.

Discussion

It is known that mice, as opposed to rats, are resistant to the diaplacental induction of neurogenic tumours by nitrosamides. Vesselinovitch *et al.* (6) described an incidence of 5.8–6.4% for ENU-induced neural tumours in C57BL × CH hybrids after treatment between g.d. 12 and 14. A comparable brain tumour frequency was also reported for ENU-treated C3HeB/FeJ mice (7). Application of 20 mg/kg ENU on g.d. 19 resulted in brain glioblastomas in 6.8% of male and 2.4% of female offspring. Wechsler *et al.* (8), analysing the data from 4555 mice offspring

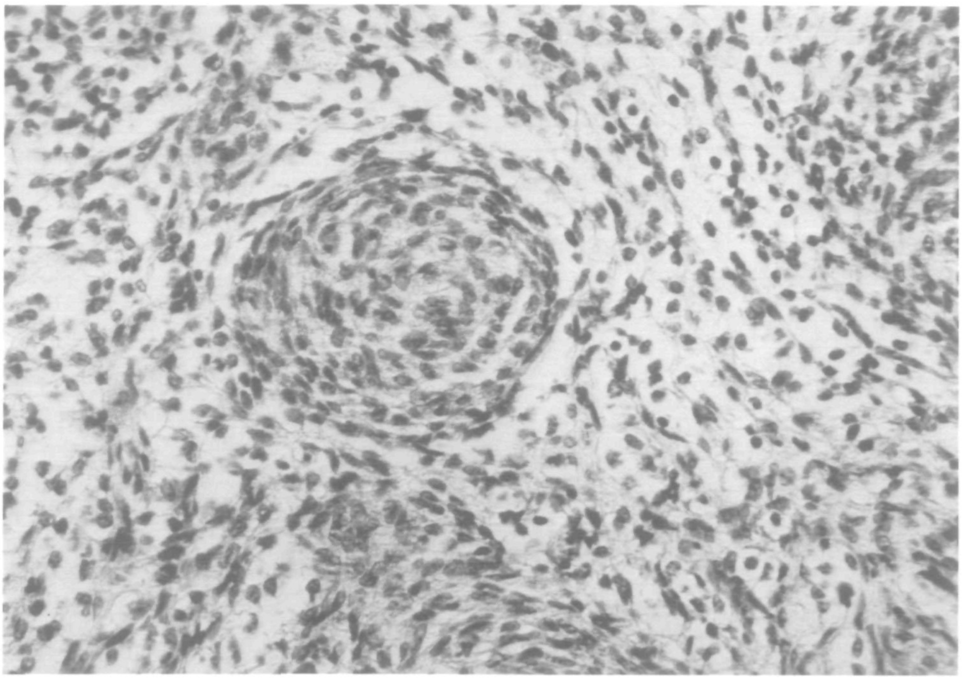

Fig. 3. Female (T × HT)F1 mouse at an age of 562 days, after ENU treatment (10 mg/kg) on g.d. 12. Meningioma with typical onion-shaped arrangement of cells forming a broad extending tumour mass between the pituitary gland and the olfactory bulbs. This tumour revealed great destructive capacity for the underlying bone. H&E, ×560.

Table IX. Incidence of tumours (number and per cent) of the CNS–skull–vertebra interface in (T × HT)F1 mice in relation to the gestation period of induction and to tumour distribution along the neuraxis (ENU groups with 40 mg/kg)

	No. of experimental animals	Tumour location			All tumours of the CNS pial border
		Skull base	Cervico-thorax segments	Lumbo-sacral segments	
Single ENU treatment within					
organogenesis period (g.d. 8–11)	520	(56) 10.8^a	(6) 1.2	(22) 4.2^b	(84) 16.2^a
fetal period (g.d. 12–14)	367	(107) 29.2^a	(9) 2.5	(37) 10.1^b	(153) 41.7^a
All treatments	887	(163) 18.4	(15) 1.7	(59) 6.7	(237) 26.7
Topographic distribution of the tumours (%)		69	6	25	

Significances between pairs of data: $^aP < 0.0001$; $^bP = 0.05$.

of the NIH-Swiss, DBA and C57B1 strains after ENU treatment between g.d. 12 and 20, observed tumours of the CNS with a frequency as low as 0.6%. Others did not observe any CNS tumours in C57B16, DBA or AKR mice after ENU treatment (9). They described, however, an incidence of 3.6–3.9% CNS tumours in SWR/J mice. Some other negative results in CNS tumour development by diaplacentally active ENU were reported for nude CBA mice (10), NMRI mice (11) and for A/J mice or for the C57B16 strain (12).

These reports indicate a low susceptibility of the sub-ependymal layer of the CNS to nitrosamide carcinogenesis in mice, a target tissue with an outstanding sensitivity in rats (13,14). In addition, the Schwann cells of the trigeminus nerve and of other parts of the peripheral nervous system have also been described as target cells of ENU effects in rats (15,16). The induction of Schwann cell tumours was, however, quite independent of the origin of meningiomas, which amounted to 1.8% in these experiments. This was of comparable magnitude to the incidence of meningosarcoma (1%) in C3H mice after ENU treatment (7). This strain was regarded as just as sensitive as most rat strains to ENU, as the frequency of Schwannoma was ~30% after treatment on g.d. 19 with 20 mg/kg ENU (1,7). Another preferential target within the CNS of Wistar, Fischer and Long–Evans rats was described for neonatal ENU treatment. In cerebellar tumours arising in these strains (17) as well as in spinal cord tumours (18), glioma stem cells were found to be situated in 93% of all cases in the sub-pial CNS periphery. Histologically, all tumours were classified as oligodendrogliomas with some occasional astrocytic foci. However, meningeal or sarcomatous tumours were not found in one single case.

In contrast to the above studies in rats, (T × HT)F1 hybrids have revealed a unique target at the border between neuroectodermal and mesodermal tissues.

An additional finding in our mice must be separated from the occurrence of tumours, namely the hyperplastic lesions of the cranial meninges which were observed both in the dorsal and basal regions of the brain. This nevertheless indicates a distinct sensitivity of the meningeal cells to a proliferation response after ENU exposure.

This characteristic carcinogenic effect of ENU at the brain–skull and spinal cord–vertebra interfaces established in this study should be emphasized with respect to the following peculiarities:

(i) These tumours were not homogeneously distributed along the neuraxis, but showed a preference for the cranial location rather than for the lumbospinal segments. Although they did not reveal any relationship with the cervico-thoracal segments, which represent the preferential stem cell region for melanoblasts, their correlation with spot induction during organogenesis, especially in female offspring, is intriguing (W.Schmahl *et al.*, submitted). It is therefore assumed that neural crest tissue is involved in carcinogenesis, but not those parts of the neural crest that form the melanocytes or other constituents of other tissues or organs. Otherwise the latter would also have revealed some carcinogenic effects.

(ii) The tumours showed a marked preference for the basal parts of the CNS. This might be related to the genetical background of the (T × HT)F1 hybrids, similar to the topographical pattern of ENU-induced lung tumours and intestinal tumours ascribed recently to distinct genetic influences (19). However, while this would explain the interface location of tumours in general, it would not explain their preference for the ventral parts of the CNS. This factor can therefore be explained more plausibly in the light of histogenetic events occurring at the base of the CNS during embryogenesis.

The neural crest cells in the cephalic region of mice arise from the lateral extremity of the neural folds on g.d. 8 (20,21). Those cells originating from the lateral and dorsal margins invade the mesenchyme, which later forms some parts of the skull skeleton (22). Most of the crest cells arising from the ventral part of this lateral lip spread out medially to invade the region of the inner brain curvature, i.e. the area of the subsequent fasciculi optici (23). Neural crest cells are not distinguishable from the primitive mesenchyme on g.d. 10 (21,24). Thereafter, the first meningeal and vascular elements are present within a cellular reticulum occupying the space between the brain and the fibrous elements of the dura to be formed later (25). Neurothelial cells, which continuously form the perineural cell sheath of nerves upon leaving the meningeal space, are first seen in the region of the later sella turica as the earliest differentiation of the primitive mesenchyme (26–28). A sudden increase of the mitotic index of those cells related to the meningeal cell investment of the region between the fascicular optici was observed by Sturrock (29,30) in rodent embryos at a stage corresponding to g.d. 9–10 in the mouse.

Most importantly, these migratory neural crest cells have been recently described to possess a striking heterogeneity in terms of their capacity for differentiation (31). This implies not only cell lineage for neurons of certain peripheral ganglia, but also satellite glial cells of such neurons, Schwann cells engulfing the nerves and mesectodermal derivatives that form connective tissue structures. These latter cell types of neural crest origin—namely glial cells, Schwann cells and connective tissue cells—are obviously the main targets for ENU-induced carcinogenesis in the present experiments with (T × HT)F1 mice. In addition, this sensitive cell population is nearly exclusively limited to the basal parts of the structures derived from the neural crest. The sensitive period starts as early as g.d. 8 in female embryos. To our knowledge no comparable experiment in mice has reported such an early induction period (32). The most significant studies by Wechsler *et al.* (8) and Vesselinovitch *et al.* (6) started with ENU applications to mice at g.d. 12. This is a rather arbitrary time schedule that does not exclude the possibility of some sensitivity to lung tumour and leukemia induction being present even earlier. Presumably this schedule was influenced by a previous detailed time–response study on ENU effects in rats (15). Ivankovic and Druckrey reported an absence of tumour induction before g.d. 12 in the rat, which would correspond to g.d. 11 in the mouse (33). Similarly, Nomura (34), when studying the diaplacental induction of lung tumours in ICR mice by urethane, did not find any effect before g.d. 11.

Besides the relatively early inducibility of CNS border zone tumours, there is obviously a developmental gradient in topographical sensitivity which presumably reflects a similar histogenetic gradient: the lumbospinal parts reveal not only the earliest carcinogenic effects but also show maximum sensitivity at the lowest dose. In contrast, tumorous late effects are exclusively concentrated at the base of the brain at the latest application time (g.d. 14) of our experiment. This result must be interpreted as a significant example of stage specificity in the carcinogenic response at a definite site, a fact which was strictly denied in earlier studies (35). So far, only Maekawa *et al.* (36) have claimed that there is a relationship between the dose of ENU and a variation of organ specificity in carcinogenesis. The latter cannot be confirmed in the present study, as our dose–response study revealed a constant affliction of the CNS–mesenchyme interface. However, in the same phase of our experiments it became evident that those regions with an early manifestation of sensitivity, such as the lumbosacral region, simultaneously show a maximum response even after the lowest dose. This exception from the normal dose–response relationship was also shown by the pioneering experiments of Ivankovic and Druckrey (15), from which it is further known that the ENU response during earlier developmental stages is more intense than during later stages. The decrease in sensitivity of the CNS border zone to carcinogenesis on g.d. 14 is nevertheless surprising, but this result obviously has to be seen together with the earlier inducibility of tumours.

On account of these pathogenetic considerations we also claim that glial tumours and their mesenchymal (sarcomatous) components are of simultaneous origin. In human pathology the recognition of the gliosarcoma as a distinct neuropathological entity has led to a number of theories pertaining to the origin of mixed tumour cell populations. Most studies have supported the hypothesis that the glioma induces the (secondary) sarcomatous transformation of the vascular endothelium and/or the perivascular adventitial cells (37–39). In contrast to those authors, we now present experimental evidence for the simultaneous carcinogenesis of both neuroepithelial and mesenchymal tissues with a presumed common stem cell. This is shown most clearly by the latency timetables establishing that the occurrence of the various types of tumour (neuroepithelial versus meningo-mesenchymal types) was not concordant in any way. A further factor also points in this direction: there was no correlation of the frequency of neuroepithelial tumours with the number of meningo-mesenchymal tumours observed in subsequent periods alone or simultaneously with neuroepithelial tumours. Such a correlation would have indicated the presence of secondary induction events.

Our determination of a common target cell is finally supported by pathogenetic considerations which are stringent only upon the basis postulated. Thus the (T × HT) cross is also a good model for studying conditions that lead to a variable pattern of histogenetic phenotypes during carcinogenesis of a common progenitor cell.

Acknowledgements

We would like to thank Ulrike Britzelmaier, Karen Hautmann, Sabine Holthaus, Elisabeth Leipold, Anna Nickl and Gabriele Silbermann for expert technical assistance. We are grateful to Ilse-Dore Adler for many invaluable discussions and for critically reading the manuscript. This study was supported by a grant from the Umweltbundesamt Berlin (contract No. 10603040).

References

1. Denlinger,R.H., Koestner,A. and Wechsler,W. (1974) Induction of neurogenic tumors in C3HeB/FeJ mice by nitrosourea derivatives: observations by light microscopy, tissue culture and electron microscopy. *Int. J. Cancer*, **13**, 559–571.
2. Vesselinovitch,S.D., Rao,K.V.N., Mihailovich,N., Rice,J.M. and Lombard, L.S. (1974) Development of broad spectrum of tumors by ethylnitrosourea in mice and the modifying role of age, sex, and strain. *Cancer Res.*, **34**, 2530–2538.
3. Neuhäuser-Klaus,A. (1981) An approach towards the standardization of the mammalian spot test. *Arch. Toxicol.*, **48**, 229–243.
4. Rorke,L.B., Giller,F.H., Davis,R.L. and Becker,L.E. (1985) Revision of the WHO classification of brain tumors. *Cancer*, **56**, 1869–1886.
5. Mennel,H.D. and Zülch,E. (1976) Tumours of the central and peripheral nervous system. In Turusov,V.S. (ed.), *Pathology of Tumours in Laboratory Animals. Vol. I. Part 2: Tumours of the Rat*, IARC Scientific Publication no. 6. IARC, Lyon, pp. 295–312.
6. Vesselinovitch,S.D., Koka,M., Rao,K.V.N., Mihailovich,N. and Rice,J.M. (1977) Prenatal multicarcinogenesis by ethylnitrosourea in mice. *Cancer Res.*, **37**, 1822–1828.
7. Anderson,L.M., Hagiwara,A., Kovatch,R.M., Rehm,S. and Rice,J.M. (1989) Transplacental initiation of liver, lung neurogenic, and connective tissue tumors by N-nitroso compounds in mice. *Fund. Appl. Toxicol.*, **12**, 604–620.
8. Wechsler,W., Rice,J.M., Vesselinovitch,S.D. and Arat,T. (1974) Perinatale Tumorinduktion mit Äthylnitrosoharnstoff: Ein Beitrag zur Frage der Organotropie alkylierender Resorptivkanzerogene bei verschiedenen Mäusestämmen. *Verh. Deutsch. Gesellsch. Pathol.*, **58**, 546.
9. Diwan,A. and Meier,H. (1974) Strain and age-dependent transplacental carcinogenesis by 1-ethyl-1-nitrosourea in inbred strains of mice. *Cancer Res.*, **34**, 764–770.
10. Stutman,O. (1978) Spontaneous, viral, and chemically induced tumors in the nude mouse. In Fogh,J. and Giovanella,B. (eds), *The Nude Mouse in Experimental and Clinical Research*. Academic Press, New York, pp. 411–435.
11. Schmahl,W. and Kriegel,H. (1978) Oncogenic properties of transplacentally acting ethylnitrosourea in NMRI-mice after antecedent X-irradiation. *Z. Krebsforsch.*, **91**, 69–79.
12. Rice,J.M. (1979) *Perinatal Carcinogenesis*, National Cancer Institute Monograph 51. US Department of Health, Education and Welfare, Bethesda, MD, p. 35.
13. Wessel,H., Gerlach,H., Schreiber,D., Rath,F.W. and Peschel,B. (1978) Frühstadien experimenteller Hirntumoren bei Ratten. Untersuchungen an Serienschnitten. *Zbl. Allg. Pathol.*, **122**, 204–213.
14. Naito,M., Narro,Y. and Ito,A. (1981) Spinal cord tumors induced by *N*-ethyl-*N*-nitrosourea in rats: presence of spinal subpial target cells. *J. Natl. Cancer Inst.*, **72**, 715–721.
15. Ivankovic,S. and Druckrey,H. (1968) Transplacentare Erzeugung maligner Tumoren des Nervensystems. I. Äthyl-nitroso-harnstoff (ÄNH) an BD IX-Ratten. *Z. Krebsforsch.*, **71**, 320–360.
16. Zülch,K.J. and Mennel,H.D. (1971) Die Morphologie der durch alkylierende Substanzen erzeugten Tumoren des Nervensystems. *Zbl. Neurochir.*, **32**, 225–244.
17. Naito,M., Naito,Y., Fujioka,Y. and Ito,A. (1986) Morphological and immunohistochemical evidence for the presence of subcortical target cells of *N*-ethyl-*N*-nitrosourea-induced cerebellar tumors in rats. *Cancer Res.*, **46**, 5836–5841.
18. Naito,M., Naito,Y., Ito,A., Watanabe,H. and Kawashima,K. (1984) Spinal cord tumors induced by *N*-ethyl-*N*-nitrosourea in rats: presence of spinal subpial target cells. *J. Natl. Cancer Inst.*, **72**, 715–721.
19. Oomen,L.C.J.M., Valk,M.A., van der Hart,A.A.M., Demant,P. and Emmelot,P. (1988) Influence of mouse major histocompatibility complex (H-2) on *N*-ethyl-nitrosourea-induced tumor formation in various organs. *Cancer Res.*, **48**, 6634–6641.
20. Rawles,M.E. (1947) Origin of pigment cells from the neural crest in the mouse embryo. *Physiol. Zool.*, **20**, 248–266.
21. Bartelmez,G.W. (1960) Neural crest from the forebrain in mammals. *Anat. Rec.*, **138**, 269–281.
22. Morris,G.M. and Thorogood,P.U. (1978) An approach to cranial neural crest cell migration and differentiation in mammalian embryos. In Johnson,M.H. (ed.), *Development in Mammals*. North-Holland, Amsterdam, Vol. 3, pp. 363–412.
23. Nichols,D.H. (1981) Neural crest formation in the head of the mouse embryo as observed using new histological techniques *J. Embryol. Exp. Morphol.*, **64**, 105–120.
24. McLone,D G. and Bondareff,W. (1975) Developmental morphology of the subarachnoid space and contiguous structures in the mouse. *Am. J. Anat.*, **162**, 273–294.
25. Weston,J.A. (1970) The migration and differentiation of neural crest cells. *Adv. Morphogenet.*, **8**, 41–114.
26. Andres,K.H. (1967) Über die Feinstruktur der Arachnoidea und Dura mater von Mammalia. *Z. Zellforsch.*, **79**, 272–295.
27. Seitz,R., Löhler,J. and Schwendemann,G. (1981) Ependyma and meninges of the spinal cord of the mouse. *Cell Tissue Res.*, **220**, 61–72.
28. Kusakabe,M., Sakakura,T., Sano,M. and Nishizuka,Y. (1984) Early development of mouse anterior pituitary: role of mesenchyme. *Dev. Growth Different.*, **26**, 263–271.
29. Sturrock,R.R. (1987) A quantitative histological study of cell division and changes in cell number in the meningeal sheath of the embryonic human optic nerve. *J. Anat.*, **155**, 133–140.
30. Sturrock,R.R. (1988) An ultrastructural study of the development of leptomeningeal macrophages in the mouse and rabbit. *J. Anat.*, **156**, 207–215.
31. Baroffio,A., Dupin,E. and Le Douarin,N.M. (1988) Clone-forming ability and differentiation potential of migratory neural crest cells. *Proc. Natl. Acad. Sci. USA*, **85**, 5325–5329.
32. Mohr,U., Emura,M. and Richter-Reichhelm,H.B. (1980) Transplacental carcinogenesis. *Invest. Cell. Pathol.*, **3**, 209–229.
33. Schneider,B.F. and Norton,St. (1979) Equivalent ages in rat, mouse and chick embryos. *Teratology*, **19**, 273–278.

34. Nomura,T. (1974) An analysis of the changing urethan response of the developing mouse embryo in relation to mortality, malformation, and neoplasm. *Cancer Res.*, **34**, 2217–2231.
35. Alexandrov,V.A. and Napalkov,N.P. (1981) General regularities of transplacental (prenatal) carcinogenesis. *Biol. Res. Pregnancy*, **2**, 181–187.
36. Maekawa,A., Ociu,T., Matsuoka,Ch., Onodera,H , Furuta,K., Kurokawa,Y., Takahashi,M., Kokubo,T., Tanicawa,H., Hayashi,Y., Nakadate,M. and Tanimura,A. (1984) Carcinogenicity of low doses of *N*-ethyl-*N*-nitrosourea in F344 rats, a dose-response study. *Gann*, **75**, 117–125.
37. Rubinstein,L.J. (1956) The development of contiguous sarcomatous and gliomatous tissue in intracranial tumours. *J. Pathol. Bacteriol.*, **71**, 441–459.
38. Feigin,I., Ransohoff,J. and Liebermann,A. (1976) Sarcoma arising in oligodendroglioma of the brain. *J. Neuropathol. Exp. Neurol.*, **35**, 679–684.
39. Slowik,F., Jellinger,K., Gaszo,L. and Fischer,J. (1985) Gliosarcoma: histological, immunohistochemical, ultrastructural, and tissue culture studies. *Acta Neuropathol.*, **67**, 201–220.

Received on January 15, 1990; revised on May 10, 1990; accepted on May 21, 1990